

# INTERNAL STRUCTURE DAMAGE EVOLUTION IN COMPOSITE USING SYNCHROTRON RADIATION

Xiaofang Hu Xiaoping Wu \*<sup>1</sup>

(University of Science and Technology of China, Key Laboratory of Mechanical Behavior and Design of Materials, Chinese Academy of Sciences, Hefei Anhui, 230027, China)

## ABSTRACT

In this paper SR light is used for the observation of internal structure and damage evolution in composite material by three kinds of techniques: (1) Scanning X-ray microscopy, (2) X-ray Absorbing Imaging, and (3) X-ray Computed Tomography. By Scanning X-ray Microscopy, a silicon thin plate with thickness of 0.5mm was detected by soft X-ray. The resolution of scanning image was 2 $\mu$ m. With X-ray Absorbing Imaging technique, epoxy resin matrix composite reinforced by single boron fiber undergone tensile loading was observed. Also, the damage evolution for Bi-2223/ Ag HTS (high temperature superconducting) tapes at 77K under tensile loading were investigated with the same method. In order to obtaining the 3-D internal structures, the X-ray Computed Tomography technique was used to inspecting the internal topology of sintering ceramics.

## 1. INTRODUCTION

Synchrotron radiation (SR) source produces intense, tunable, monochromatic, and highly collimated beam, it is suitable to examining the innermost structures of opaque materials by measuring the X-ray energy transmitted through the materials. The X-ray transmission attenuation values are directly related to material's constituents and are a function of the atomic number. It is useful to feature detection, density measurements, constituent identification, and dimensional measurements [1-9].

Comparing with conventional optical microscopy or SEM, SR technique does not require polished surfaces or serial sections. It has the advantage for nondestructive observation of internal structures in materials. Combining with different approaches and selecting proper X-ray energy, it can detect various materials.

## 2. EXPERIMENTS AND DISCUSSION

### (1) Scanning X-ray Microscopy

This experiment was performed at microscopy beam line of Hefei National

---

\*<sup>1</sup> Corresponding author: Xiaoping Wu, Department of Mechanics and Mechanical Engineering, University of Science and Technology of China, Hefei Anhui, 230027, China. Tel: +86-551-3601248; Fax: +86-551-3631760; E-mail: xpwu@ustc.edu.cn

Synchrotron Radiation Laboratory (NSRL). A thickness of 0.5mm silicon thin plate, which was broken by laser impact, was examined by means of scanning X-ray microscopy. The SR X-ray was converged as a small spot to impinge on the specimen that was held on two-dimensional precision movable stage. First of all SR source was separated into monochromatic X-ray by interferometer and the wavelength  $32 \text{ \AA}$  was selected. Then it was further focused to a micro spot by micro Fresnel zoneplate to scan the specimen point by point and the transmitted X-ray was detected by photon-counter to give the digital image. With this wavelength the transparency of specimen is good and the contrast is high between silicon and voids on image. The internal damage of silicon plate was shown in Fig.1 and Fig.2. The received photon numbers described the cracks and voids with different height and color. The high cliff in Fig.1 or red strip in Fig.2 represented the crack about  $10\mu\text{m}$  width. There were many voids in front of the main crack, and tended to link together to form the new crack. The image resolution was depended on the size of focused spot. It was  $2\mu\text{m}$  in this experiment. The scanning area was  $50\mu\text{m} \times 50\mu\text{m}$ .

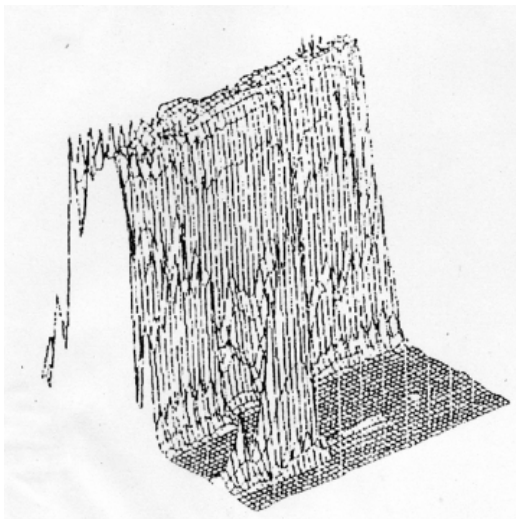


Fig.1 3-D drawing for internal damage of silicon plate

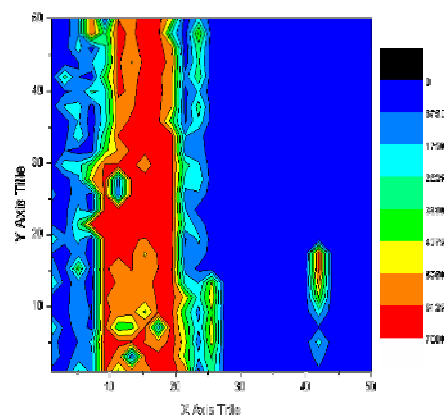


Fig.2 2-D drawing shown damage with color

## (2) X-ray Absorbing Imaging

The X-ray absorbing imaging technique used wide spectrum X-rays coming from SR source. The X-rays were directly projected on to material specimen. The transmission rays were recorded by photo-resist PMMA or X-ray film.

In order to observe the structure damage evolution, a special tensile stage was designed for the tension of specimen. Tensile pull-off tests were performed on epoxy resin matrix reinforced by boron fiber at lithography beam line of NSRL. A  $0.3(\text{W}) \times 0.3(\text{T}) \times 20(\text{L})$ -mm specimen was examined. The boron-fiber was  $130\mu\text{m}$  in diameter and covered with carbon layer in  $20\mu\text{m}$  thick. The experiment was done in the vacuum chamber. The wavelength of X-rays was  $5 \text{ \AA} \sim 20 \text{ \AA}$ . The PMMA photo-resist was used to record the image. The flaw, damage accumulation and cracks growth at interface between fiber core and cover were observed during the fiber suffered tension, Fig.3. It could be seen that there were original defects at

interface 1 and 2 (Fig.3-a). During loading, the defects developed into a group of micro cracks, and expanded towards the fiber core. Furthermore, new micro-cracks 3 were produced in the vicinity (Fig.3-b). With the increase of load, the micro-cracks developed continuously (Fig.3-c).

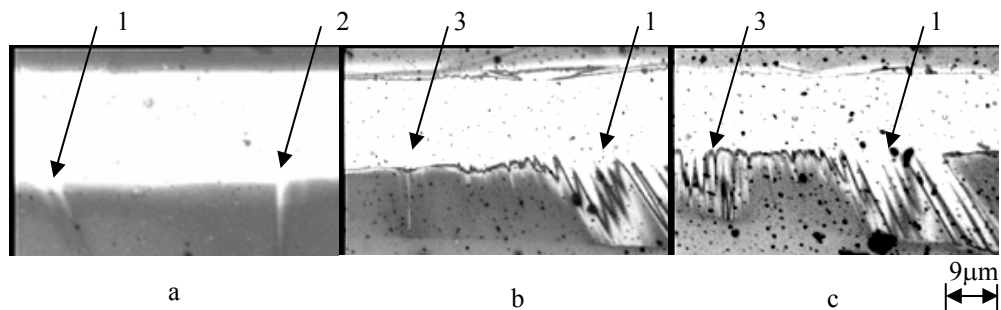


Fig.3 Damage evolution at interface between cover and fiber core

Another experiment on the observation of internal structure damage evolution in Bi-2223/Ag HTS (high temperature superconducting) tape at 77K under tensile loading had been done at the X-ray tomography beam line of Beijing Synchrotron Radiation Facility (BSRF). The X-ray wavelength range of the beam line is  $0.3 \text{ \AA} \sim 2.5 \text{ \AA}$ . The monofilament tape was chosen to perform the experiment, and it was composed of oxide core  $\text{Bi}_2\text{Sr}_2\text{Ca}_2\text{Cu}_3\text{O}_x$  with Ag sheath. The specimen dimensions were about  $3.3(\text{W}) \times 0.2(\text{T}) \times 26(\text{L})\text{-mm}$ . At beginning, the tape kept linear elasticity. The critical current density  $J_c$  was almost as  $J_{c0}$  as constant (as shown in Fig.5). With the increase of load, the tape came into plastic flow refer to the yield point (Fig.4-b, Fig.5 at point  $\sigma_1$ ). The microcracks initiated in core and ran cross the tape. Critical current density  $J_c$  decreased dramatically after this point. The tape began to lose superconducting capability. Increasing load sequentially, the microcracks became more and more until the microcracks assembled to macro penetrable transverse one. Finally the tape was fractured.

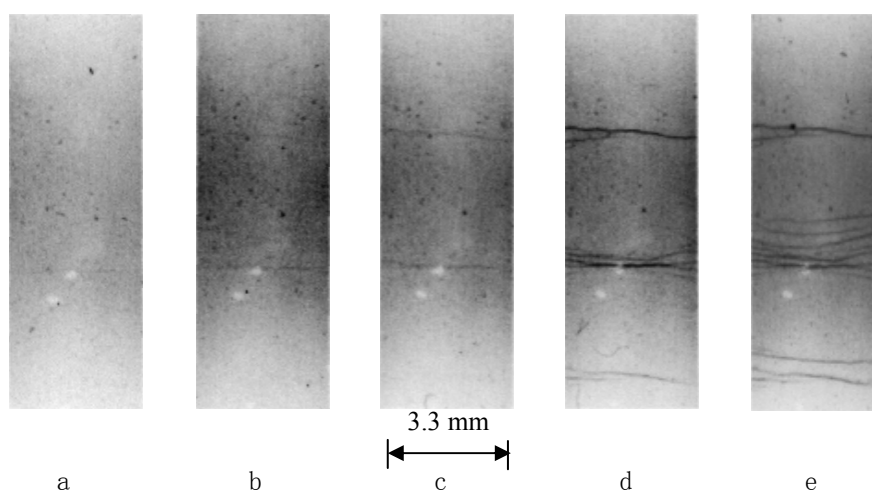


Fig.4 Damage evolution photographs of monofilament Bi-2223/Ag tape at 77K

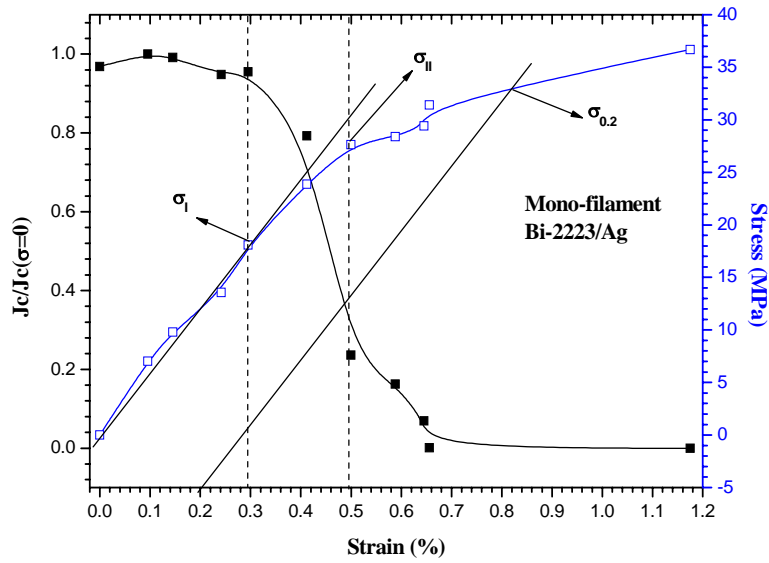


Fig. 5  $J_c/J_{c0}$ -strain-stress curve of monofilament Bi-2223/Ag tape

### (3) X-ray Computed Tomography

The SR-CT system had been developed to image material structures nondestructively in three dimensions. Parallel X-rays pass through a specimen positioned on a rotation stage, then are recorded by high resolution X-ray film (better than  $2\mu\text{m}$ ). The specimen is rotated by a small angle, and another two-dimensional absorption image is obtained. This process continues until  $180^\circ$  of specimen rotation has been recorded. Reconstruction software with convolution re-projection arithmetic converts X-ray absorption profile data into two-dimensional reconstructions of the linear attenuation coefficients in the specimen interior. These values are rendered into three-dimensional view.

The sintered porous ceramics was investigated by SR-CT. With this technique 3-D pore geometrical topology, quantitative pore ratio and average density were obtained. The experiment was also performed at X-ray tomography beam line of BSRF. An X-ray of wavelength  $1.34 \text{ \AA}$  was selected for projection. The photon flux at  $\lambda=1.34 \text{ \AA}$  was  $6 \times 10^{10} \text{ photons s}^{-1} \text{ mA}^{-1} \text{ mrad}^{-2} \text{ 0.1\% BW}^{-1}$ . Specimen was a sintered ceramic cylinder with diameter of 5mm. The sintering temperature was  $1200^\circ\text{C}$ . The composition of the ceramics is shown in Table-1. Project images were recorded at  $2^\circ$  intervals, and 90 images were obtained for 3-D reconstruction.

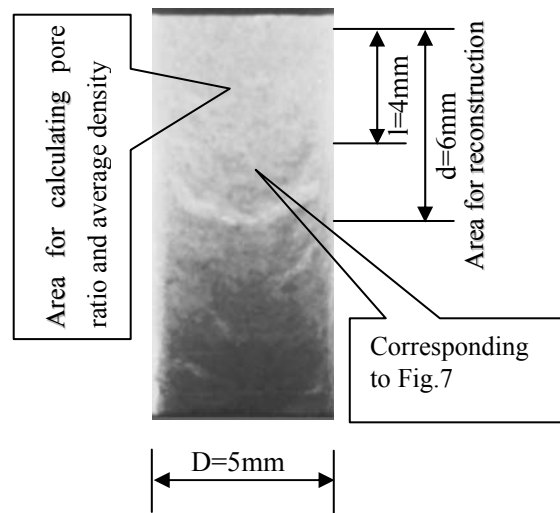


Fig.6 Projection slice at  $0^\circ$

Fig.6 shows a single projection slice at angle  $0^\circ$ . The part of length 6mm was

chosen for reconstruction, and 4mm for calculating pore ratio and average density. The reconstruction topologies of cross section for different layer were given in Fig.7. It was corresponding to the 2mm part in Fig.6. The innermost pores, their distribution and changes along longitude were clearly shown. The resolution of reconstruction image was about 10 $\mu$ m. The elements and their mass attenuation coefficients of the specimen were given in table-2.

**Table-1** Composition lists

Composition (i)	Mass ratio (R <sub>i</sub> )
SiO <sub>2</sub>	75.8%
Al <sub>2</sub> O <sub>3</sub>	1.05%
Na <sub>2</sub> O	14.7%
CaO	8.4%

**Table-2** Elements and mass attenuation coefficients

Elements (i)	Mass ratio (R <sub>i</sub> )	Mass Attenuation coefficients ( $\mu_i / \rho_i$ )
<i>Si</i>	35.43%	0.0448
<i>Al</i>	0.56%	0.0431
<i>Na</i>	10.91%	0.0427
<i>Ca</i>	6.0%	0.0451
<i>O</i>	47.1%	0.0444

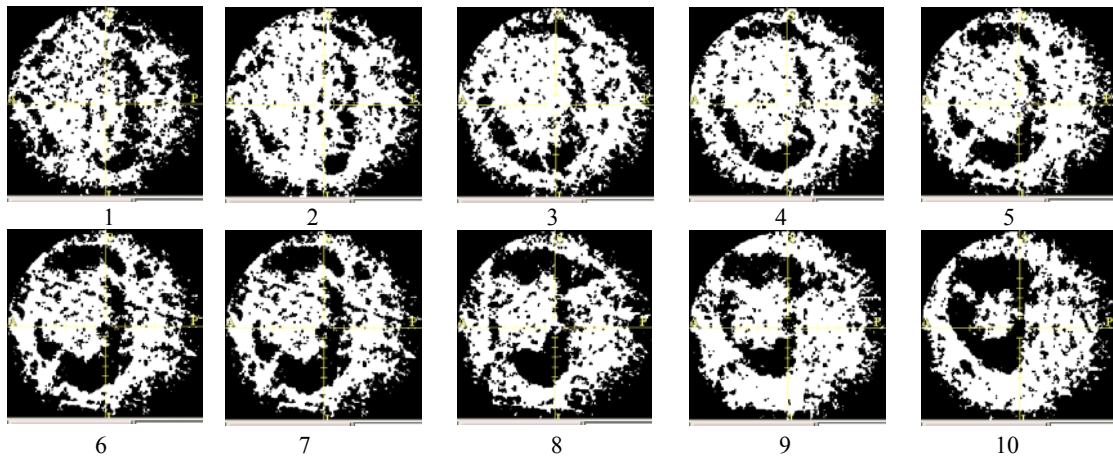


Fig.7 Section topology of different layer

Calculation for pore ratio  $\varepsilon$  was based on formula (1)

$$\varepsilon = \frac{N \left( \mu(i, j) \Big|_{\mu(i, j) \cong \mu_{air}} \right)}{N \left( \mu(i, j) \right)} \times 100 \% \quad (1)$$

$N( )$  and  $\mu(i, j)$  represented sum of pixels and reconstruction linear attenuation coefficient at pixel (i, j) respectively. According to the reconstruction results, the calculated value of pore ratio was 35.74% in volume.

To obtain the average density, the total average mass attenuation coefficient ( $\mu/\rho$ ) should

be calculated according to formula (2).

$$\frac{\mu}{\rho_{total}} = \sum_i \frac{\mu_i}{\rho_i} R_i \quad (2)$$

$\rho$  is density and  $R$  is mass ratio. The calculated result was as following.

$$\frac{\mu}{\rho_{total}} = \sum_{i,j} \frac{\mu(i,j)}{\rho(i,j)} = 0.04439 \text{ g/cm}^2 \quad (3)$$

According to formula (3), the average density of the specimen was calculated as  $\rho = 2.26 \text{ g/cm}^3$ . It was agreement with the value which was measured by Archimedes method  $\rho = 2.04 \text{ g/cm}^3$ . Error was within the 9.7%.

### 3. CONCLUSIONS

SR X-ray is a powerful tool to inspect material nondestructively. By the monochromatic synchrotron radiation, it is possible to unambiguously measure the absolute values of the X-ray attenuation coefficient for the different structures in the materials. With the development of high resolution recording transducer and SR techniques, it would take an important role in the materials observation. The availability of such experimental data should have a profound effect on the modeling of damage evolution in composites and other advanced materials.

### ACKNOWLEDGEMENTS

This work was performed under the support of National Nature Science Foundation of China under Contract No. 10232030 and BSRF Foundation. The authors would like to thank Dr. Jinglei Yang, Dr. Xiaoning Jing and Prof. Yulian Tian at BSRF for their contribution for this work.

### References:

1. Richard H. Bossi and Gary E. Georgeson, Composite structure development decision using X-ray CT measurements, *Material Evaluation* (1995)1198-1203.
2. T.Hirano and K.Usami, In situ x-ray CT under tensile loading using synchrotron radiation, *J. Mater. Res.*, Vol. 10, No.2 (1995), 381-386.
3. J.H.Kinney et al, Nondestructive investigation of damage in composites using X-ray tomography (XTM), *J.Mateer.Res.*Vol.5 (1990), 1123-1129.
4. E. Maire, L. Babout, J.Y. Buffiere, R. Fougères, Recent results on 3D characterization of microstructure and damage of metal matrix composites and a metallic foam using X-ray tomography, *Materials Science and Engineering*, A319-321 (2001) 216-219
5. Lame, D.Bellet, M.Di Michiel, D.Bouvard, Bulk observation of metal powder sintering by X-ray synchrotron microtomography, *Acta Materialia*, 2004 (in press)
6. B. L. Illman et al, Synchrotron Applications In forestry and forest products, *Synchrotron*

Radiation News, Vol.10 (1997), 18-23.

7. P.Munshi, M.Maisl, H.Reiter, A new method of characterizing patterns in X-ray tomographic images of a composites specimen, Nuclear. Instruments. And Methods. In Physics Research B 108. (1996), 205-212.
8. George Y. Baaklini, Ramakrishna T. Bhatt, et al, X-ray microtomography of ceramic and metal matrix composites, Materials Evaluation, (1995), 1040-1044.
9. U. Bonse, X-ray tomography microscopy of fibre-reinforced Materials, J. Mater. Sci., 26(1991), 4076-4085
10. Y. Nagata et al, High Energy High Resolution Monochromatic X-ray Computed Tomography Using The Photo Factory Vertical Wiggler Beamline, Rev. Sci. Instrum., 63(1), (1992), 615-618.
11. W. B. Lindquist et al, Medial axis analysis of void structure in three-dimensional tomography images of porous media, J. Geophys. Res., 101(B4), (1996), 8297-8310.
12. M.Suenaga, Y.Fukumoto, P.Haldar, T.R.Thurston and U.Wildgrüber, Effects of axial tensile and bending strains on critical currents of mono- and multicored (Bi,Pb)<sub>2</sub>Sr<sub>2</sub>Ca<sub>2</sub>Cu<sub>3</sub>O<sub>10</sub>-Ag tapes, Appl. Phys.Lett, 67 (1995), 3025
13. K.Kawano,S.Isosa,A.Oota.,Physica C, Study of current distribution in Ag-Bi2223 tape using a scanning Hall-Probe. Magnetometry, Vol. 2289, (1997), 282-287.